

where B_j and C_j are constant (Noda, Kasatani, Watanabe & Terauchi, 1992). B_j for S, K(2) and O(2) is calculated, $B_S = 1.446 \times 10^{-3}$, $B_K = 2.709 \times 10^{-3}$, $B_O = 4.142 \times 10^{-3} \text{ \AA}^2$ and also C_j for these atoms, $C_S = 6.272 \times 10^{-22}$, $C_K = 7.593 \times 10^{-22}$, $C_O = 9.087 \times 10^{-22} \text{ J}$. The solid lines in Fig. 4 are the calculated values from (5). The mean square amplitude $\langle u_j^2 \rangle$ at 0 K refers to the zero-point motion. The temperature dependence of the mean square amplitude $\langle u_j^2 \rangle$ is explained by (5) throughout the temperature region investigated in the present work. No anomaly is seen for the temperature dependence of the mean square amplitude $\langle u_j^2 \rangle$.

Concluding remarks

The crystal structure of potassium sulfate was investigated at temperatures from 296 down to 15 K, using a four-circle diffractometer. Throughout the temperature region investigated in the present work, the crystal structure is found to be orthorhombic, space group *Pmcn*. Unit-cell volume and lattice constants decrease monotonously as temperature decreases. The temperature dependence of the unit-cell volume and the lattice constants is explained by the Grüneisen relation. Atomic positions of K(1), K(2) and S move to the special position of the α -K₂SO₄ structure as temperature increases. The S—O bond lengths in SO₄ tetrahedra do not alter as temperature changes. The temperature dependence of mean square amplitude $\langle u_j^2 \rangle$ decreases monotonously as temperature decreases and is explained by (5). Both

the unit-cell volume and the mean square amplitude $\langle u_j^2 \rangle$ show no anomaly to indicate a phase transition below room temperature.

The authors thank Mr Y. Kitamura for the growth of single crystals. We are also indebted to Professor H. Mashiyama at Yamaguchi University for his kind offer of the program AXS89 system.

References

- ADAMS, L. H. & GIBSON, U. R. E. (1931). *J. Wash. Acad.* **21**, 381–390.
 ARNOLD, H., KURTZ, W., RICHTER-ZINNIUS, A., BETHKE, J. & HEGER, G. (1981). *Acta Cryst.* **B37**, 1643–1651.
 BERG, A. J. VAN DEN & TUINSTRRA, F. (1978). *Acta Cryst.* **B34**, 3177–3181.
 COCHRAN, W. (1973). *The Dynamics of Atoms in Crystals*. London: Edward Arnold Ltd.
 CRUICKSHANK, D. W. J. (1956a). *Acta Cryst.* **9**, 754–756.
 CRUICKSHANK, D. W. J. (1956b). *Acta Cryst.* **9**, 757–758.
 EL-KABBANY, F. A. I. (1980). *Phys. Status Solidi A*, **58**, 373–378.
 GESI, K., TOMINAGA, Y. & URABE, H. (1982). *Ferroelectr. Lett.* **44**, 71–75.
 HASEBE, K., MASHIYAMA, H., TANISAKI, S. & GESI, K. (1984). *J. Phys. Soc. Jpn.* **53**, 1866–1868.
 IZUMI, M., AXE, J. D. & SHIRANE, G. (1977). *Phys. Rev. B*, **15**, 4392–4411.
 MASHIYAMA, H. (1991). *J. Phys. Soc. Jpn.* **60**, 180–187.
 MCGINNETY, J. A. (1972). *Acta Cryst.* **B28**, 2845–2852.
 MIYAKE, M., MORIKAWA, H. & IWAI, S. (1980). *Acta Cryst.* **B36**, 532–536.
 NODA, Y., KASATANI, H., WATANABE, Y. & TERAUCHI, H. (1992). *J. Phys. Soc. Jpn.* **61**, 905–915.
 PINNOCK, P. R., TAYLOR, C. A. & LIPSON, H. (1956). *Acta Cryst.* **9**, 173–178.
 ROBINSON, M. T. (1958). *J. Phys. Chem.* **62**, 925–928.
 SAWADA, A., TANAKA, K., MATSUMOTO, H. & NISHIHATA, Y. (1995). *Ferroelectrics*. To be published.
 UNRUH, H. G. (1970). *Solid State Commun.* **8**, 1951–1954.

Acta Cryst. (1995). **B51**, 293–300

Two 9,10-Anthracenocryptand Silver(I) Nitrate Complexes. Fluorescence Modulated by Ag⁺ as a Function of the Geometry of the Complex

BY H. ANDRIANATOANDRO, Y. BARRANS AND P. MARSAU

Laboratoire de cristallographie et Physique cristalline, URA 144 CNRS, Université de Bordeaux I, 33405 Talence CEDEX, France

AND J. P. DESVERGNE, F. FAGES AND H. BOUAS-LAURENT

Laboratoire de Photophysique et Photochimie Moléculaire, URA 348 CNRS, Université de Bordeaux I, 33405 Talence CEDEX, France

(Received 17 January 1994; accepted 12 October 1994)

Abstract

The two anthracenocryptands 3,12-octano-3,12-diaza-6,9,31,34-tetraoxa[14](9,10)anthracenophane, C₃₀H₄₀N₂O₄ (A₂₂), and 4,13-octano-4,13-diaza-7,10,33,36-tetraoxa[6](9,10)anthracenophane,

C₃₂H₄₄N₂O₄ (A₃₃), were designed to direct interactions between π -electrons and Ag⁺. In each complex displaying 1:1 stoichiometry, Ag⁺ is encapsulated in the cavity of the cryptand and coordinated to O and N atoms of the diaza-crown ether. In (A₂₂)/Ag⁺ complex (I), Ag⁺ lies at a Ag⁺–anthracene mean plane distance of 3.01 Å. Two

conformations of the silver complex (IIA) and (IIB) are observed in the crystal lattice of $(A_{33})/Ag^+$, with different distances (5.14 and 4.46 Å) between Ag^+ and the anthracene plane. The fluorescence properties of the crystals reflect the difference in geometry between $(A_{22})/Ag^+$ and $(A_{33})/Ag^+$. The fluorescence spectra were recorded at room temperature with a Hitachi-Perkin-Elmer MPF44 fluorimeter corrected for emission and excitation. The same single crystals were used both for X-ray structure determination and fluorescence emission studies. The fluorescence is collected in a direction at right angles to the beam of the exciting light.

Introduction

Anthracenocryptands (A_{22} and A_{33} , see Fig. 1) were designed (Fages *et al.*, 1988, 1989; Guinand *et al.*, 1986; Marsau *et al.*, 1988) to study the interaction between the anthracene ring and diverse metal cations encapsulated just above the central aromatic ring. Moreover, as the 'N₂O₄' complexing subunit is separated from the aromatic ring by two chains of different lengths, one could anticipate a modification of the fluorescence properties of the system with the distance between the cation and anthracene.

It was already shown that light metal cations and protons induce strong modifications of the fluorescence emission spectra by inhibiting intramolecular exciplex formation between the N atoms and the aromatic ring (Fages *et al.*, 1989); nevertheless, the electronic absorption spectra in methanol solutions undergo little alteration. In contrast, heavy metal cations, in particular Ag^+ , display hypochromism and bathochromic effects in absorption spectra, characteristic of charge transfer (CT) complexes in the ground state.

Ag^+ is known to smoothly coordinate with π -electrons and specifically to usually display an η^2 hapticity with

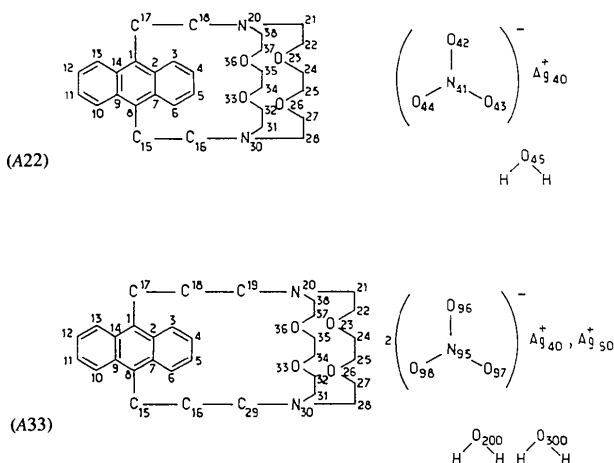


Fig. 1. Formula and crystallographic numbering of the two anthracenocryptands (A_{22}) and (A_{33}), including Ag^+ and NO_3^- ions. The numbering of conformer (II) of (A_{33}) is obtained by addition of 50 to the numbering of conformer (I).

Table 1. Crystal data, data collection and refinement parameters for (I) and (II)

Crystal data	(I)	(II)
Chemical formula	$C_{30}H_{40}N_2O_4 \cdot AgNO_3 \cdot H_2O$	$C_{32}H_{44}N_2O_4 \cdot AgNO_3 \cdot 0.5H_2O$
Solvent	Chloroform/toluene	Chloroform/toluene
Crystal system	Monoclinic	Monoclinic
Space group	$P2_1/c$	$C2/c$
M_r	679.6	699.6
a (Å)	10.479 (1)	34.545 (1)
b (Å)	15.751 (1)	10.035 (1)
c (Å)	19.177 (1)	38.188 (2)
β (°)	110.20 (1)	98.83 (1)
Z	4	16
D_x ($Mg\ m^{-3}$)	1.520	1.421
V (Å ³)	2968.88 (5)	13081.3 (5)
$F(000)$	1416	5840
μ (cm^{-1})	59.5	54.8
Crystal size (mm)	$0.05 \times 0.4 \times 0.7$	$0.05 \times 0.3 \times 1.5$
Data collection		
Cu $K\alpha$ radiation (Å)	1.5418	1.5418
No. of reflections	25	21
2θ range (°)	87–97	80–95
Temperature (K)	Room (≈ 295)	Room (≈ 295)
Intensity measurements		
h	0–13	–36–31
k	0–19	0–0
l	–23–22	0–40
Total no. of reflections measured	6340	8717
Empirical absorption correction	$T = 1.0-0.674$	$T = 1.0-0.874$
No. of observed reflections [$I \geq 3\sigma(I)$]	497	4214
Structure refinement		
No. of parameters	546	580
R [$I \geq 3\sigma(I)$]	0.054	0.094
wR	0.041	0.092
S	1.34	1.53
$\Delta\rho$ ($e\ \text{Å}^{-3}$)	–0.3–0.5	–0.4–0.5

aromatic compounds (Andrews, 1954; Andrews & Keefer, 1964; Probst, Stiegelmann, Reide & Schmidbaur, 1991); for example, in the anthracene tetrasilver(I) complex the cation is linked to the side ring bonds (Hall & Amma, 1969; Griffith & Amma, 1974*a,b*). Even when the Ag^+ cation could fit into an electron-rich cavity, for instance in the deltaphane (Cohen-Addad, Baret, Chautemps & Pierre, 1983; Kang, Hanson, Eaton & Boekelheide, 1985), it remains outside the cage and coordinates with two benzene bonds. Therefore, it seemed appropriate to investigate the crystal structures of $(A_{22})/Ag^+$ (I) and $(A_{33})/Ag^+$ (II) complexes in order to demonstrate the inside position of silver. This will be the basis of explaining the fluorescence-emitting properties of the anthracene ring as a function of the structure.

Crystal structure determinations

Both (I) and (II)

Crystal structures were solved by the heavy-atom method (see Tables 1). The Ag^+ cation position was obtained from the Patterson map and the rest of the

non-H atoms from subsequent Fourier recycles; the atomic positions of the nitrate anion and the location of one (A_{22}) or two (A_{33}) molecules of water as inclusion were determined by Fourier-difference maps. A disorder was identified in the O atoms of the NO_3^- moiety; non-H atoms were first refined with isotropic thermal factors and then the H-atom positions were calculated; Ag, C, N and O atoms were refined anisotropically using block-diagonal least-squares. The same single crystals were used both for X-ray structure determinations and fluorescence emission studies (see Table 2 for atomic parameters).*

(A_{22})/Ag⁺ (I)

The Ag⁺ ion is encaged inside the cavity of (A_{22}) (Fig. 2). The conformation of the complexing crown is *in-in* (the electronic lone pairs on the two N atoms are pointing inside the cavity, toward the cation). A comparison between the free ligand (Guinand *et al.*, 1986) and (I) shows that some distances and torsion angles of the diaza-crown ether subunit are modified, except around the C—C bonds. The distances between the O atoms (crossly opposed on either side of the chain) inversely vary after complexation, *e.g.* O(23)···O(33) increases from 5.80 to 5.99 Å, and O(26)···O(36) decreases from 5.55 to 4.55 Å. The N···N distance differs very slightly (5.04 Å rather than 5.18 Å for the free ligand), as opposed to (A_{22})/Tl⁺ (Hinschberger, 1988) where it takes a value of 6.00 Å. This value is 4.92 Å for the Ag⁺ [2.2.2]cryptate (Hilgenfeld & Saenger, 1982).

* Lists of structure factors and H-atom coordinates have been deposited with the IUCr (Reference: PA0297). Copies may be obtained through The Managing Editor, International Union of Crystallography, 5 Abbey Square, Chester CH1 2HU, England.

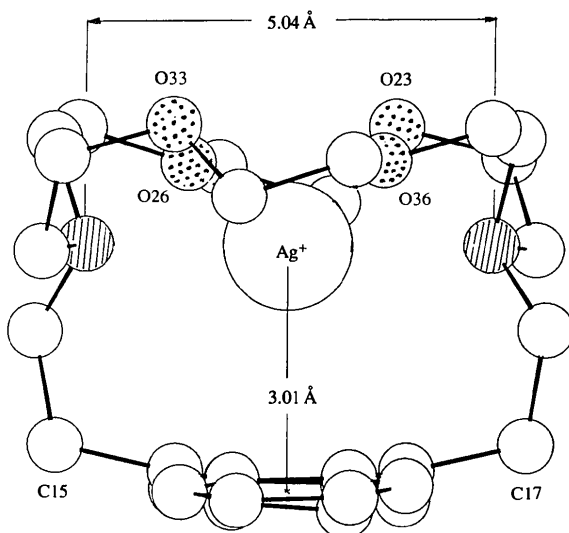


Fig. 2. Molecular structure of the (A_{22})/Ag⁺ complex in the crystal; view along the long axis of the anthracene ring.

Table 2. Atomic positional parameters for (A_{22})/Ag⁺ and (A_{33})/Ag⁺

$$B_{eq} = (4/3) \sum_i \sum_j \beta_{ij} a_i a_j$$

	x	y	z	B_{eq}
(A_{22})/Ag ⁺				
Ag(40)	-0.02834 (2)	0.16746 (2)	0.08705 (2)	3.70 (1)
C(1)	-0.0107 (5)	0.3456 (3)	0.1657 (2)	2.8 (2)
C(2)	0.1183 (5)	0.3146 (3)	0.2092 (2)	2.9 (2)
C(3)	0.2423 (5)	0.3564 (3)	0.2128 (2)	3.6 (2)
C(4)	0.3655 (5)	0.3252 (4)	0.2552 (3)	4.1 (2)
C(5)	0.3751 (5)	0.2490 (4)	0.2946 (3)	4.2 (2)
C(6)	0.2612 (5)	0.2071 (3)	0.2942 (2)	3.6 (2)
C(7)	0.1287 (4)	0.2384 (3)	0.2534 (2)	2.9 (2)
C(8)	0.0093 (5)	0.1979 (3)	0.2551 (2)	2.8 (2)
C(9)	-0.1152 (5)	0.2383 (3)	0.2234 (2)	2.9 (2)
C(10)	-0.2370 (5)	0.2097 (3)	0.2349 (2)	3.4 (2)
C(11)	-0.3564 (5)	0.2496 (4)	0.2037 (3)	4.3 (2)
C(12)	-0.3690 (5)	0.3211 (4)	0.1579 (3)	4.5 (2)
C(13)	-0.2584 (5)	0.3512 (3)	0.1443 (3)	3.9 (2)
C(14)	-0.1275 (5)	0.3122 (3)	0.1767 (2)	2.9 (2)
C(15)	0.0212 (5)	0.1095 (3)	0.2871 (2)	3.3 (2)
C(16)	0.0579 (5)	0.0446 (3)	0.2372 (2)	3.7 (2)
C(17)	-0.0264 (5)	0.4102 (3)	0.1055 (2)	3.4 (2)
C(18)	-0.0928 (5)	0.3698 (3)	0.0277 (2)	3.7 (2)
N(20)	-0.0185 (4)	0.2973 (2)	0.0115 (2)	3.3 (2)
C(21)	0.1165 (5)	0.3278 (4)	0.0135 (3)	4.2 (2)
C(22)	0.1980 (6)	0.2683 (4)	-0.0168 (3)	4.5 (3)
O(23)	0.2103 (3)	0.1835 (2)	0.0114 (2)	4.0 (2)
C(24)	0.2983 (5)	0.1773 (4)	0.0865 (3)	4.6 (2)
C(25)	0.3002 (5)	0.0878 (4)	0.1101 (3)	4.6 (2)
O(26)	0.1642 (4)	0.0663 (2)	0.1033 (2)	4.5 (2)
C(27)	0.1496 (6)	-0.0188 (3)	0.1237 (3)	5.2 (3)
C(28)	0.0056 (6)	-0.0300 (3)	0.1214 (3)	4.4 (2)
N(30)	-0.0411 (4)	0.0375 (2)	0.1602 (2)	3.3 (2)
C(31)	-0.1743 (5)	0.0127 (3)	0.1645 (3)	4.3 (2)
C(32)	-0.2807 (6)	-0.0180 (3)	0.0933 (3)	4.8 (3)
O(33)	-0.3040 (4)	0.0384 (2)	0.0322 (2)	4.3 (2)
C(34)	-0.3747 (6)	0.1131 (4)	0.0374 (3)	4.9 (3)
C(35)	-0.3811 (5)	0.1693 (4)	-0.0261 (3)	4.5 (2)
O(36)	-0.2449 (3)	0.1892 (2)	-0.0207 (2)	3.9 (1)
C(37)	-0.2398 (6)	0.2446 (3)	-0.0780 (3)	4.3 (2)
C(38)	-0.0946 (6)	0.2653 (3)	-0.0646 (2)	4.0 (2)
O(45)	0.3301 (5)	0.0462 (3)	0.4451 (3)	8.4 (3)
N(41a)*	-0.4104 (13)	0.0406 (5)	0.3487 (5)	10.1 (8)
N(41b)*	-0.3715 (15)	0.0229 (6)	0.3826 (4)	8.9 (6)
O(42a)*	-0.3210 (9)	0.0567 (5)	0.3411 (4)	12.1 (5)
O(42b)*	-0.3203 (17)	0.0531 (11)	0.3313 (9)	15.4 (11)
O(43)†	-0.4461 (9)	0.0695 (5)	0.4021 (5)	18.5 (6)
O(44a)*	-0.5041 (31)	0.0291 (17)	0.3048 (14)	22.1 (17)
O(44b)	-0.3511 (21)	-0.0327 (12)	0.4107 (16)	6.2 (17)
(A_{33})/Ag ⁺				
Conformer (IIA)				
Ag(40)	0.63734 (3)	0.0542 (1)	0.09702 (3)	3.65 (4)
C(1)	0.7077 (4)	-0.058 (2)	0.2017 (3)	3.9 (7)
C(2)	0.6965 (4)	0.068 (2)	0.2149 (4)	4.1 (8)
C(3)	0.7233 (5)	0.182 (2)	0.2205 (4)	4.9 (9)
C(4)	0.7128 (5)	0.298 (2)	0.2345 (5)	6.0 (10)
C(5)	0.6744 (6)	0.311 (2)	0.2424 (4)	6.0 (10)
C(6)	0.6468 (5)	0.212 (2)	0.2364 (4)	4.3 (8)
C(7)	0.6579 (5)	0.087 (2)	0.2211 (4)	3.9 (8)
C(8)	0.6282 (4)	-0.011 (2)	0.2111 (4)	3.8 (8)
C(9)	0.6424 (4)	-0.139 (2)	0.2040 (4)	3.7 (8)
C(10)	0.6161 (5)	-0.254 (2)	0.1983 (4)	5.0 (10)
C(11)	0.6297 (6)	-0.378 (2)	0.1940 (5)	6.0 (10)
C(12)	0.6700 (5)	-0.395 (2)	0.1938 (4)	5.0 (10)
C(13)	0.6975 (5)	-0.294 (2)	0.1978 (4)	5.3 (9)
C(14)	0.6827 (4)	-0.161 (2)	0.2018 (3)	3.0 (7)
C(15)	0.5856 (5)	0.024 (2)	0.2037 (4)	4.4 (8)
C(16)	0.5746 (4)	0.054 (2)	0.1634 (4)	4.3 (7)
C(17)	0.7442 (4)	-0.063 (2)	0.1837 (4)	5.1 (9)
C(18)	0.7312 (5)	-0.025 (2)	0.1432 (4)	5.2 (9)
C(19)	0.7098 (5)	-0.140 (2)	0.1240 (4)	4.7 (9)
N(20)	0.6855 (3)	-0.104 (1)	0.0898 (3)	3.7 (6)

Table 2 (cont.)

	x	y	z	B_{eq}
C(21)	0.6656 (5)	-0.227 (2)	0.0743 (5)	5.1 (9)
C(22)	0.6304 (5)	-0.275 (2)	0.0933 (4)	5.0 (10)
O(23)	0.5998 (3)	-0.180 (1)	0.0904 (3)	4.5 (5)
C(24)	0.5756 (5)	-0.189 (2)	0.0574 (5)	5.3 (9)
C(25)	0.5496 (5)	-0.067 (2)	0.0536 (4)	5.0 (8)
O(26)	0.5734 (3)	0.044 (1)	0.0503 (3)	4.2 (5)
C(27)	0.5556 (5)	0.171 (2)	0.0544 (4)	5.0 (9)
C(28)	0.5536 (5)	0.197 (2)	0.0943 (4)	4.9 (9)
C(29)	0.5888 (5)	0.188 (2)	0.1550 (4)	4.3 (8)
N(30)	0.5925 (3)	0.209 (1)	0.1167 (3)	4.0 (6)
C(32)	0.6519 (6)	0.354 (2)	0.1258 (5)	6.0 (10)
C(31)	0.6096 (5)	0.345 (2)	0.1132 (4)	4.3 (8)
O(33)	0.6740 (3)	0.282 (1)	0.1047 (3)	5.0 (6)
C(34)	0.6791 (6)	0.341 (2)	0.0718 (6)	6.0 (10)
C(35)	0.6980 (5)	0.245 (2)	0.0501 (5)	6.0 (10)
O(36)	0.6709 (3)	0.132 (1)	0.0415 (3)	4.8 (6)
C(37)	0.6891 (5)	0.015 (2)	0.0317 (4)	4.5 (8)
C(38)	0.7117 (5)	-0.054 (2)	0.0650 (4)	4.9 (8)
Conformer (IIB)				
Ag(50)	0.44701 (4)	0.0969 (2)	0.61872 (3)	5.73 (7)
C(51)	0.3062 (5)	0.270 (2)	0.6008 (5)	6.0 (10)
C(52)	0.3191 (5)	0.404 (2)	0.6103 (4)	5.1 (9)
C(53)	0.3189 (5)	0.505 (3)	0.5843 (5)	7.0 (10)
C(54)	0.3322 (7)	0.628 (3)	0.5954 (6)	8.0 (10)
C(55)	0.3454 (7)	0.659 (3)	0.6325 (7)	8.0 (10)
C(56)	0.3471 (5)	0.569 (2)	0.6569 (5)	6.0 (10)
Conformer (IIB) and nitrate groups				
C(57)	0.3325 (4)	0.432 (2)	0.6470 (4)	4.7 (8)
C(58)	0.3318 (5)	0.333 (2)	0.6730 (4)	4.6 (8)
C(59)	0.3135 (5)	0.214 (2)	0.6641 (5)	5.3 (9)
C(60)	0.3067 (7)	0.122 (3)	0.6913 (7)	8.0 (10)
C(61)	0.2927 (7)	-0.003 (3)	0.6827 (8)	10.0 (20)
C(62)	0.2797 (7)	-0.035 (3)	0.6496 (8)	10.0 (20)
C(63)	0.2833 (6)	0.044 (3)	0.6190 (7)	9.0 (20)
C(64)	0.2998 (5)	0.177 (2)	0.6269 (6)	6.0 (10)
C(65)	0.3560 (5)	0.345 (2)	0.7094 (5)	6.0 (10)
C(66)	0.3911 (5)	0.243 (2)	0.7140 (4)	6.0 (10)
C(67)	0.3018 (5)	0.229 (3)	0.5619 (5)	7.0 (10)
C(68)	0.3439 (9)	0.232 (4)	0.5491 (7)	11.0 (20)
C(69)	0.3740 (6)	0.188 (3)	0.5719 (8)	9.0 (20)
N(70)	0.4108 (4)	0.138 (2)	0.5612 (4)	5.3 (8)
C(71)	0.4310 (6)	0.241 (2)	0.5423 (5)	6.0 (10)
C(72)	0.4470 (6)	0.356 (2)	0.5656 (6)	7.0 (10)
O(73)	0.4786 (4)	0.294 (2)	0.5905 (4)	7.3 (8)
C(74)	0.4980 (7)	0.388 (3)	0.6150 (6)	8.0 (10)
C(75)	0.5278 (6)	0.321 (2)	0.6402 (5)	7.0 (10)
O(76)	0.5101 (3)	0.217 (1)	0.6585 (3)	6.3 (7)
C(77)	0.4949 (5)	0.261 (3)	0.6910 (5)	7.0 (10)
C(78)	0.4724 (6)	0.149 (2)	0.7027 (5)	7.0 (10)
C(79)	0.4063 (5)	0.222 (2)	0.6768 (4)	4.8 (9)
N(80)	0.4374 (4)	0.117 (2)	0.6791 (3)	5.0 (7)
C(81)	0.4217 (6)	-0.014 (2)	0.6905 (5)	6.0 (10)
C(82)	0.4410 (8)	-0.128 (3)	0.6779 (7)	9.0 (20)
O(83)	0.4292 (4)	-0.137 (2)	0.6390 (4)	7.6 (8)
C(84)	0.4502 (8)	-0.242 (3)	0.6248 (8)	9.0 (20)
C(85)	0.4417 (6)	-0.231 (2)	0.5859 (6)	7.0 (10)
O(86)	0.4589 (3)	-0.105 (1)	0.5771 (3)	6.2 (7)
C(87)	0.4448 (5)	-0.062 (3)	0.5405 (5)	6.0 (10)
C(88)	0.4061 (5)	0.015 (2)	0.5400 (5)	6.0 (10)
N(95)	0.4398 (4)	0.399 (4)	0.2663 (8)	15 (2)
O(96)	0.451 (1)	0.500 (4)	0.253 (1)	19 (3)
O(97)	0.413 (1)	0.450 (4)	0.287 (1)	19 (3)
O(98)	0.4704 (8)	0.368 (3)	0.2938 (8)	16 (2)
N(295)	0.3636 (8)	0.642 (3)	0.5055 (8)	13 (2)
O(296)	0.3330 (8)	0.557 (3)	0.4954 (7)	15 (2)
O(297)	0.3911 (7)	0.585 (3)	0.5129 (8)	16 (2)
O(298)	0.3564 (8)	0.750 (3)	0.5156 (7)	15 (2)
O(300)*	0.253 (4)	0.595 (5)	0.464 (1)	12 (3)
O(400)*	0.433 (1)	0.486 (3)	0.469 (1)	11 (4)

* Occupancy factor 0.5.

† Occupancy factor 1.0.

Table 3. Bond lengths (Å) and angles (°) involving Ag⁺

(I)			
Ag(40)—N(20)	2.526 (4)	N(20)—Ag(40)—N(30)	179.0 (1)
Ag(40)—N(30)	2.510 (4)	N(20)—Ag(40)—O(23)	60.0 (1)
Ag(40)—O(23)	3.304 (4)	N(20)—Ag(40)—O(26)	113.3 (1)
Ag(40)—O(26)	2.502 (4)	N(20)—Ag(40)—O(33)	120.4 (1)
Ag(40)—O(33)	3.387 (4)	N(20)—Ag(40)—O(36)	67.8 (1)
Ag(40)—O(36)	2.510 (3)	N(30)—Ag(40)—O(23)	120.1 (1)
		N(30)—Ag(40)—O(26)	66.9 (1)
		N(30)—Ag(40)—O(33)	58.7 (1)
		N(30)—Ag(40)—O(36)	111.4 (1)
Ag(40)—C(1)	3.162 (5)	O(23)—Ag(40)—O(26)	53.4 (1)
Ag(40)—C(2)	3.277 (5)	O(23)—Ag(40)—O(33)	127.0 (1)
Ag(40)—C(7)	3.241 (5)	O(23)—Ag(40)—O(36)	103.5 (1)
Ag(40)—C(8)	3.146 (5)	O(26)—Ag(40)—O(33)	102.7 (1)
Ag(40)—C(9)	3.249 (5)	O(26)—Ag(40)—O(36)	130.4 (1)
Ag(40)—C(14)	3.235 (5)	O(33)—Ag(40)—O(36)	52.8 (1)
(IIA)			
Ag(40)—N(20)	2.35 (1)	N(20)—Ag(40)—N(30)	168.6 (5)
Ag(40)—N(30)	2.40 (1)	N(20)—Ag(40)—O(23)	74.7 (4)
Ag(40)—O(23)	2.68 (1)	N(20)—Ag(40)—O(26)	115.6 (4)
Ag(40)—O(33)	2.61 (1)	N(20)—Ag(40)—O(33)	105.4 (4)
Ag(40)—O(26)	2.62 (1)	N(20)—Ag(40)—O(36)	72.7 (4)
Ag(40)—O(36)	2.68 (1)	N(30)—Ag(40)—O(23)	105.7 (4)
		N(30)—Ag(40)—O(26)	73.8 (4)
		N(30)—Ag(40)—O(33)	74.4 (4)
		N(30)—Ag(40)—O(36)	116.0 (4)
Ag(40)—C(1)	4.49 (2)	O(23)—Ag(40)—O(26)	63.6 (3)
Ag(40)—C(2)	4.65 (2)	O(23)—Ag(40)—O(33)	179.1 (4)
Ag(40)—C(7)	4.69 (2)	O(23)—Ag(40)—O(36)	116.2 (4)
Ag(40)—C(8)	4.46 (2)	O(26)—Ag(40)—O(33)	117.0 (4)
Ag(40)—C(9)	4.50 (2)	O(26)—Ag(40)—O(36)	83.9 (4)
Ag(40)—C(14)	4.60 (1)	O(33)—Ag(40)—O(36)	64.9 (4)
(IIB):			
Ag(50)—N(70)	2.39 (2)	N(70)—Ag(50)—N(80)	137.9 (5)
Ag(50)—N(80)	2.39 (2)	N(70)—Ag(50)—O(73)	71.2 (5)
Ag(50)—O(73)	2.57 (2)	N(70)—Ag(50)—O(76)	133.9 (5)
Ag(50)—O(76)	2.74 (1)	N(70)—Ag(50)—O(83)	108.5 (5)
Ag(50)—O(83)	2.58 (2)	N(70)—Ag(50)—O(86)	71.8 (5)
Ag(50)—O(86)	2.65 (1)	N(80)—Ag(50)—O(73)	118.0 (5)
		N(80)—Ag(50)—O(76)	69.1 (5)
		N(80)—Ag(50)—O(83)	73.2 (5)
		N(80)—Ag(50)—O(86)	134.6 (5)
Ag(50)—C(51)	5.11 (2)	O(73)—Ag(50)—O(76)	62.7 (5)
Ag(50)—C(58)	5.32 (2)	O(73)—Ag(50)—O(83)	164.3 (5)
Ag(50)—C(52)	5.36 (2)	O(73)—Ag(50)—O(86)	102.8 (5)
Ag(50)—C(59)	5.30 (2)	O(76)—Ag(50)—O(83)	116.2 (5)
Ag(50)—C(57)	5.42 (2)	O(76)—Ag(50)—O(86)	119.1 (4)
Ag(50)—C(64)	5.20 (2)	O(83)—Ag(50)—O(86)	63.2 (5)

The Ag⁺ ion is coordinated to four heteroatoms [O(26), O(36), N(20) and N(30)] of the diaza-crown ether and six C atoms of the central aromatic ring. The O(26)···Ag⁺···O(36) and N(20)···Ag⁺···N(30) angles are 130.4 and 179.0°, respectively. The latter value has been clearly reported for other macrocyclic (Ferguson, McCrindle & Parquez, 1984; Aoki & Saenger, 1984) and silver complexes. The four distances, two Ag⁺···N and two Ag⁺···O, are almost equivalent, exhibiting the mean value of 2.51 and 2.50 Å, respectively (Table 3). These distances are considerably less than the sum of the silver(I) ionic radius and the N or O van der Waals radii [2.84 and 2.77 Å (Pauling, 1969)], and comparable with the usual values found in the literature for macrocycles (Louis, Pélassard & Weiss, 1976; Linqvist, 1957; Vranka & Amma, 1966; Wiest & Weiss, 1973), indicating the partial covalent character of these bonds. The Ag⁺ ion is held in the close vicinity of the centre of the ring at

3.01 Å from the anthracene mean plane, lying on the sixfold pseudo-axis with $\text{Ag}^+\cdots\text{C}$ distances varying from 3.15 to 3.28 Å, with a hapticity of 6 with respect to the aromatic cycle.

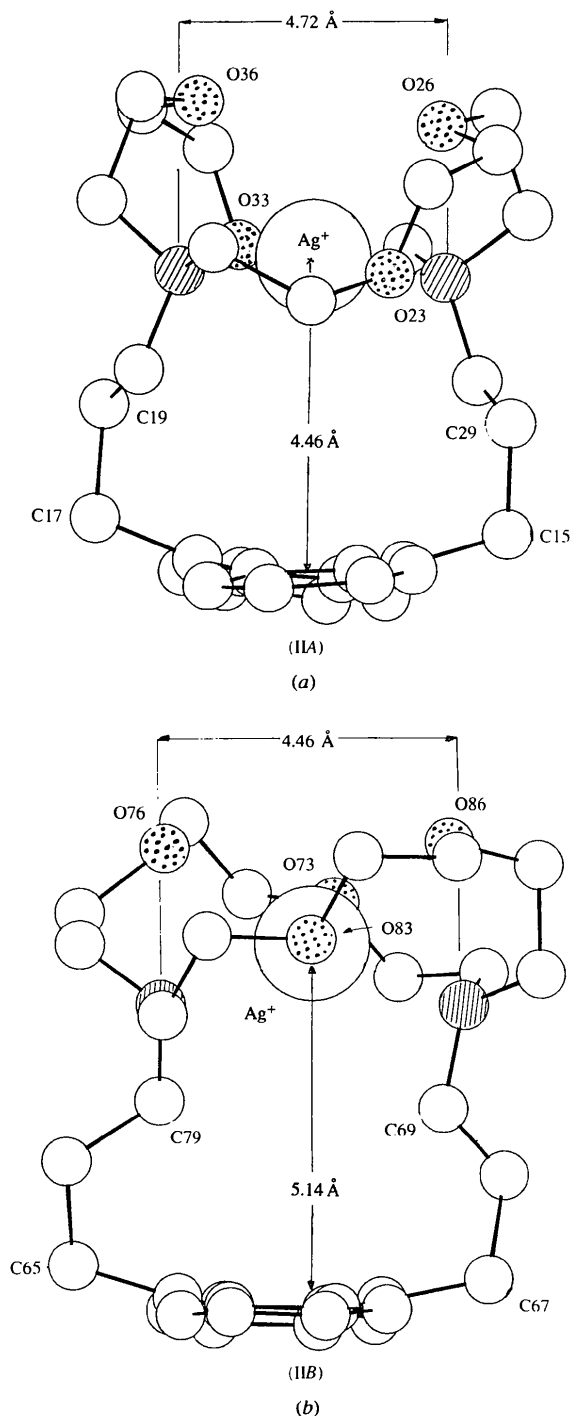


Fig. 3. Molecular structure of the two $(A_{33})/\text{Ag}^+$ complexes within the same single crystal; view along the long axis of the anthracene ring.

$(A_{33})/\text{Ag}^+$ (II)

There are two independent complexed entities (IIA) and (IIB) in the asymmetric unit cell. For (I), the Ag^+ cations are in the centre of the cavities of the complexing hosts, both in (IIA) and (IIB) conformers (Fig. 3). Unlike the previously observed free ligand (A_{33}) [*out-in* conformation (Guinand *et al.*, 1986)], both the complexes adopt an *in-in* conformation. A detailed analysis of the distances between heteroatoms and dihedral angles shows significant differences between the two conformers (IIA) and (IIB). The $\text{N}\cdots\text{N}$ distance 6.17 Å for the free ligand decreases to 4.72 and 4.46 Å for (IIA) and (IIB), respectively. The electron lone pairs of the same O atoms [O(23), O(33) and O(73), O(83)] in each conformer are oriented towards the cation.

For (IIA) and (IIB) conformers, the metallic ion is coordinated with the six heteroatoms of the complexing subunit. The $\text{Ag}^+\cdots\text{N}$ distances are almost equivalent in both conformations and range between 2.35 and 2.40 Å (Table 3); as previously observed for (I), these distances are considerably less than the sum of the Ag^+ ionic radius and the N atom van der Waals radius. They underline the covalent character of these bonds and are comparable to those found in pyridinophane macrocycle complexes (Reddy, Ravichandran, Chacko, Weber & Saenger, 1989; Drew, Rice & Silong, 1984). Weak $\text{Ag}^+\cdots\text{O}$ interactions are observed with distances varying from 2.57 to 2.74 Å in both cryptates. This emphasizes that the Ag^+ cation has a smaller affinity for the O atom than for the N atom (Christensen, Hill & Izatt, 1971). The Ag^+ cation is located at 4.46 and 5.14 Å from the mean plane of the anthracene ring in cryptates (IIA) and (IIB), respectively. Therefore, there are only weak contacts between the π -electronic cloud of the aromatic nucleus and the Ag^+ ion. The complexing subunit is too far away from the anthracene ring for any strong interactions with Ag^+ [in contrast to $(A_{22})/\text{Ag}^+$]. Following the position of Ag^+ with regard to the aromatic moiety, the (A_{33}) ligand displays different arrangements: either by a conformational modification of the lateral bridges of the complexing crown, or by a more or less important perturbation of the alkyl lateral chains due to their length. A shrinkage of the cavity is observed in the (IIB) conformer at the C(69) and C(79) positions [$d(\text{C}\cdots\text{C}) = 4.0$ Å instead of 5.60 Å in (IIA)]. Moreover, the presence of two different conformations for the cryptate within the same crystal is quite an unusual phenomenon [see Table 4 for C—C, C—O and C—N bond lengths in (I), (IIA) and (IIB)].

Anion environment and interactions

In both compounds, the ionic pair Ag^+NO_3^- is broken: $d(\text{Ag}^+\cdots\text{NO}_3^-) > 8.0$ and 5.6 Å for (I) and (II), respectively. The bond lengths and angles (Table 5) of the three nitrate groups are quite irregular compared with

Table 4. Bond lengths (Å) and angles (°) for $(A_{22})/Ag^+$ and $(A_{33})/Ag^+$ (conformers IIA and IIB)

	$(A_{33})/Ag^+$	
	Conformer (IIA)	Conformer (IIB)
$(A_{22})/Ag^+$		
C(1)—C(2)	1.407 (5)	1.438 (21)
C(1)—C(14)	1.413 (5)	1.349 (19)
C(1)—C(17)	1.505 (6)	1.527 (22)
C(2)—C(3)	1.437 (6)	1.464 (22)
C(2)—C(7)	1.451 (6)	1.399 (21)
C(3)—C(4)	1.358 (6)	1.354 (25)
C(4)—C(5)	1.403 (6)	1.411 (26)
C(5)—C(6)	1.362 (6)	1.371 (24)
C(6)—C(7)	1.425 (6)	1.461 (21)
C(7)—C(8)	1.414 (6)	1.431 (21)
C(8)—C(9)	1.389 (6)	1.410 (20)
C(8)—C(15)	1.510 (6)	1.498 (21)
C(9)—C(10)	1.440 (6)	1.470 (22)
C(9)—C(14)	1.447 (6)	1.426 (19)
C(10)—C(11)	1.341 (6)	1.344 (25)
C(11)—C(12)	1.406 (7)	1.404 (26)
C(12)—C(13)	1.358 (6)	1.380 (25)
C(13)—C(14)	1.433 (6)	1.446 (22)
C(15)—C(16)	1.537 (6)	1.553 (22)
C(16)—N(30)	1.488 (6)	
C(16)—C(29)		1.488 (22)
C(29)—N(30)		1.499 (20)
C(17)—C(18)	1.549 (6)	1.591 (24)
C(18)—N(20)	1.474 (6)	
C(18)—C(19)		1.499 (24)
C(19)—N(20)		1.486 (20)
N(20)—C(21)	1.481 (6)	1.494 (20)
N(20)—C(38)	1.490 (6)	1.493 (20)
C(21)—C(22)	1.513 (7)	1.580 (24)
C(22)—O(23)	1.429 (6)	1.420 (20)
O(23)—C(24)	1.420 (6)	1.406 (20)
C(24)—C(25)	1.478 (7)	1.512 (24)
C(25)—O(26)	1.426 (6)	1.408 (19)
O(26)—C(27)	1.420 (6)	1.426 (20)
C(27)—C(28)	1.503 (7)	1.560 (24)
C(28)—N(30)	1.474 (6)	1.482 (21)
N(30)—C(31)	1.478 (6)	1.501 (20)
C(31)—C(32)	1.512 (7)	1.471 (24)
C(32)—O(33)	1.423 (6)	1.400 (21)
O(33)—C(34)	1.412 (6)	1.423 (23)
C(34)—C(35)	1.489 (7)	1.484 (27)
C(35)—O(36)	1.428 (6)	1.474 (22)
O(36)—C(37)	1.418 (5)	1.409 (19)
C(37)—C(38)	1.489 (7)	1.545 (23)

Table 5. Bond lengths (Å) and angles (°) for nitrates in $(A_{22})/Ag^+$ and $(A_{33})/Ag^+$

$(A_{22})/Ag^+$		$(A_{33})/Ag^+$	
N(41a)—O(42a)	1.027 (15)	O(42a)—N(41a)—O(43)	124 (1)
N(41a)—O(43)	1.289 (13)	O(42a)—N(41a)—O(44a)	125 (1)
N(41a)—O(44a)	1.065 (19)	O(43)—N(41a)—O(44a)	104 (1)
N(41b)—O(42b)	1.359 (15)	O(42b)—N(41b)—O(43)	117 (1)
N(41b)—O(43)	1.220 (11)	O(42b)—N(41b)—O(44b)	128 (2)
N(41b)—O(44b)	1.012 (11)	O(43)—N(41b)—O(44b)	113 (1)
$(A_{33})/Ag^+$			
N(95)—O(96)	1.22 (5)	O(96)—N(95)—O(97)	101 (3)
N(95)—O(97)	1.38 (5)	O(96)—N(95)—O(98)	103 (3)
N(95)—O(98)	1.41 (5)	O(96)—N(95)—O(98)	97 (3)
N(295)—O(296)	1.37 (4)	O(296)—N(295)—O(297)	110 (3)
N(295)—O(297)	1.10 (4)	O(296)—N(295)—O(298)	117 (3)
N(295)—O(298)	1.17 (4)	O(297)—N(295)—O(298)	126 (4)

between anthracene groups. This is the reason why we can directly relate the results obtained by crystallographic analysis and photophysical studies in the crystal state.

Fluorescence emission spectra

Free ligands

The fluorescence emission spectra of the free ligands (A_{nn}) and their Ag^+ cryptates are shown in Fig. 4. The spectrum of the free ligand (A_{22}) exhibits a red-shifted [compared with (A_{22}) in methanol], broad, structureless band peaking at 520 nm; this emission presents a strong exciplex character (Beens & Weller, 1975; Mataga & Ottolenghi, 1979), which results from the intramolecular interaction between anthracene and the nitrogen lone pairs which are symmetrically oriented inside the cavity towards the aromatic ring (Guinand *et al.*, 1986; Marsau *et al.*, 1988). (A_{33}) displays a spectrum which deviates slightly from anthracene, the narrow emission band being centred at 465 nm. In the (A_{33}) crystal, the nitrogen lone pairs point outside the cage.

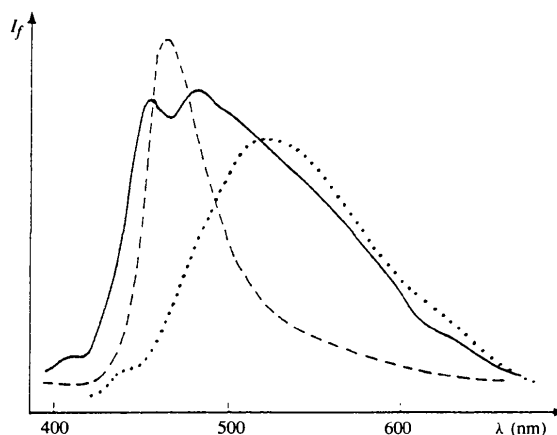


Fig. 4. Fluorescence emission spectra of (A_{22}) (.....), (A_{33}) (- - -) and $(A_{33})/Ag^+$ (—) in the crystalline state (λ_{exc} : 370 nm, room temperature). $(A_{22})/Ag^+$ single crystals were shown to be non-fluorescent.

the usual values, due to the large thermal factors. In (I) the N atom itself does not have a clearly defined position. Two statistical positions for this position, and also for atoms O(42) and O(44), were proposed from difference-Fourier maps. Their occupation factors were refined simultaneously with their thermal factors and converge to a limit close to 0.5. In (II) disorder appears for the three O atoms of the two nitrate groups (refined with large thermal motion factors). Two molecules of water were located, each with a refined occupation factor close to 0.5.

Any conformation described in this manner has to be considered with caution; thermal motion is an artificial and imperfect way to account for the disorder which affects the anion and water molecules.

Crystal packing is stabilized by van der Waals intermolecular contacts and hydrogen bonds, linking the nitrate groups and the water molecules. No significant intermolecular interactions are observed

Silver complexes

The A_{22}/Ag^+ complex was found to emit no fluorescence in the solid, in contrast to $(A_{33})/Ag^+$ which displays luminescence. The spectrum of the latter appears to be composed of two distinct emissions: a first band peaking at 455 nm with an anthracene monomeric profile and a second band, broad and red-shifted ($\lambda_{max} = 490$ nm), which may result from an exciplex (Läufer & Dreeskamp, 1986; Beens & Weller, 1975; Mataga & Ottolenghi, 1979), as suggested by that observed in solution (Fages *et al.*, 1989).

From the above-mentioned results, the following assumptions are deduced: specific Ag^+ -arene interactions could be revealed and tuned when the metal is forced by a ligand to experience a peculiar geometrical situation *versus* an aromatic nucleus. As the fluorescence properties of the $(A_{nn})/Ag$ cryptates are strongly dependent on the distance $Ag^+ \cdots$ anthracene (Ag^+ being on a line perpendicular to the middle of the central ring of the aromatic), it is tempting to establish a relationship between the geometry of the complex and the luminescence. Indeed, $(A_{22})/Ag^+$ (I) cryptate demonstrates that a *ca* 3.0 Å separation between Ag^+ and the anthracene generates a *non-fluorescent* complex, the latter being detected only in solution (Fages *et al.*, 1989) using absorption UV spectrometry (10 nm bathochromic shift on the first electronic transition, 1L_a band); the absence of fluorescence emission is probably due to a very efficient intersystem crossing (Masuhara *et al.*, 1984). $(A_{33})/Ag^+$ cryptate displays two coordination patterns for the metal, with larger distances between anthracene and the cation (4.46 and 5.14 Å). The fluorescence emission (interpreted as monomer and exciplex type bands) might be related to the structural features of the complex which present two distinct conformers. As reference materials, the single crystals of the bis-protonated cryptands [$(A_{22}), 2H^+$ and $(A_{33}), 2H^+$] display, as expected and already observed in fluid solution (Fages *et al.*, 1988, 1989), an intense fluorescence characteristic of a pure 'monomer' emission (Lahrahar, Marsau, Bouas-Laurent, Desvergne & Fages, 1994), in keeping with the following discussion. Thus, the structured emission spectrum might be ascribed to the conformer where Ag^+ is encaged on top of the cryptand, far from anthracene ($d = 5.14$ Å), and the red-shifted emission to the other conformer where the metal is closer to the π -cloud ($d = 4.46$ Å). For the latter, no steric barrier would have to be overcome to allow Ag^+ -anthracene ring overlap. Nevertheless, there is no compelling evidence for this assignment which should be considered as tentative.

Concluding remarks

9,10-Anthraceno[2.2.2]cryptands (A_{22}) and (A_{33}) were shown to form 1:1 complexes with Ag^+ ; the cation is encapsulated, being forced to adopt the unusual η^6

hapticity with the central ring of the anthracene nucleus. One of the crystals $(A_{33})/Ag^+$ presents two different conformations, a rare phenomenon, which is worth noting. The crystal fluorescence (or absence of fluorescence) might be interpreted as a function of the distance (Oevering *et al.*, 1987; Paddon-Row & Jordan, 1988) between the aromatic ring (emitter) and the silver cation (modulator), but the establishment of a precise correlation requires further investigations.

We are indebted to Professor J. M. Lehn for stimulating discussion and helpful advice.

References

- ANDREWS, L. J. (1954). *Chem. Rev.* **54**, 713–716.
 ANDREWS, L. J. & KEEFER, R. M. (1964). In *Molecular Complexes in Organic Chemistry*. San Francisco: CA: Holden Day, Inc.
 AOKI, K. & SAENGER, W. (1984). *Acta Cryst.* **C40**, 772–775.
 BEENS, H. & WELLER, A. (1975). In *Organic Molecular Photophysics*, edited by J. B. BIRKS, Vol. 2, p. 159. London: Wiley.
 CHRISTENSEN, J. J., HILL, J. O. & IZATT, R. M. (1971). *Science*, **174**, 459–467.
 COHEN-ADDAD, C., BARET, P., CHAUTEMPS, P. & PIERRE, J. L. (1983). *Acta Cryst.* **C39**, 1346–1349.
 DREW, M. G. B., RICE, D. A. & SILONG, S. B. (1984). *Acta Cryst.* **C40**, 2014–2016.
 FAGES, F., DESVERGNE, J. P., BOUAS-LAURENT, H., HINSCHBERGER, J., MARSAU, P. & PÉTRAUD, M. (1988). *New J. Chem.* **12**, 95–106.
 FAGES, F., DESVERGNE, J. P., BOUAS-LAURENT, H., MARSAU, P., LEHN, J. M., KOTZYBA-HIBERT, F., ALBRETCH-GARY, A. M. & AL-JOUBBEH, M. (1989). *J. Am. Chem. Soc.* **111**, 8672–8680.
 FERGUSSON, G., MCCRINDLE, R. & PARQUEZ, M. (1984). *Acta Cryst.* **C40**, 354–356.
 GRIFFITH, E. A. H. & AMMA, E. L. (1974a). *J. Am. Chem. Soc.* **96**, 743–749.
 GRIFFITH, E. A. H. & AMMA, E. L. (1974b). *J. Am. Chem. Soc.* **96**, 5407–5413.
 GUINAND, G., MARSAU, P., LEHN, J. M., KOTZYBA-HIBERT, F., KONOPELSKI, J. P., CASTELLAN, A., DESVERGNE, J. P., FAGES, F. & BOUAS-LAURENT, H. (1986). *Acta Cryst.* **C42**, 715–719.
 HALL, E. A. & AMMA, E. L. (1969). *J. Am. Chem. Soc.* **91**, 6538–6540.
 HILGENFELD, R. & SAENGER, W. (1982). *Topics Curr. Chem.* **101**, 1–82.
 HINSCHBERGER, J. (1988). Thèse, Université de Bordeaux I.
 KANG, H. C., HANSON, A. W., EATON, B. & BOEKELHEIDE, V. (1985). *J. Am. Chem. Soc.* **107**, 1979–1985.
 LAHRAHAR, N., MARSAU, P., BOUAS-LAURENT, H., DESVERGNE, J. P. & FAGES, F. (1994). *Acta Cryst.* Submitted.
 LÄUFER, A. G. E. & DREESKAMP, H. (1986). *Ber. Bunsenges. Phys. Chem.* **90**, 1195–1199.
 LINQVIST, I. (1957). *Acta Cryst.* **10**, 29–32.
 LOUIS, R., PÉLISSARD, D. & WEISS, R. (1976). *Acta Cryst.* **B32**, 1480–1485.
 MARSAU, P., BOUAS-LAURENT, H., DESVERGNE, J. P., FAGES, F., LAMOTTE, M. & HINSCHBERGER, J. (1988). *Mol. Cryst. Liq. Cryst.* **156**, 383–392.
 MASUHARA, H., SHIOYAMA, H., SAITO, T., HAMADA, K., YASOSHIMA, S. & MATAGA, N. (1984). *J. Phys. Chem.* **88**, 5868–5873.
 MATAGA, N. & OTTOLENGHI, M. (1979). In *Molecular Association*, edited by R. FOSTER, Vol. 2. London: Academic Press.
 OEVERING, H., PADDEN-ROW, M. N., HEPPENER, M., OLIVER, A. M., COTSARIS, E., VERHOEVEN, J. W. & HUSH, N. S. (1987). *J. Am. Chem. Soc.* **109**, 3258–3269.
 PADDON-ROW, M. N. & JORDAN, K. D. (1988). In *Modern Models of Bonding Delocalization*, edited by J. F. LIEBMAN & A. GREENBERG, p. 116. Weinheim: VCH Publishers.

PAULING, P. (1969). *The Nature of the Chemical Bond*, 2nd ed. pp. 164–179, 346. Ithaca: Cornell Univ. Press.
 PROBST, T., STIEGELMANN, O., REIDE, J. & SCHMIDBAUR, H. (1991). *Chem. Ber.* **124**, 1089–1093.

REDDY, J. P., RAVICHANDRAN, V., CHACKO, K., WEBER, E. & SAENGER, W. (1989). *Acta Cryst.* **C45**, 1871–1874.
 VRANKA, R. G. & AMMA, E. L. (1966). *Inorg. Chem.* **5**, 1020–1025.
 WIEST, R. & WEISS, R. (1973). *J. Chem. Soc. Chem. Commun.* pp. 678–679.

Acta Cryst. (1995). **B51**, 300–307

More Space-Group Changes

BY RICHARD E. MARSH

The Beckman Institute, California Institute of Technology, Pasadena, CA 91125, USA*

AND IVAN BERNAL

Department of Chemistry, University of Houston, Houston, TX 77204-5641, USA

(Received 9 June 1994; accepted 18 October 1994)

Abstract

Revisions are made to the space groups in ten published X-ray diffraction studies. In five cases the revisions entail increases in the Laue symmetry and, except for repositioning a nitrate group in one compound, there are no important changes in the interatomic distances and angles. In four other cases, centers of symmetry have been added; in one of these cases further refinement has led to appreciable changes in the bond lengths and angles, while in the other three cases the original intensity data were not available and further refinement could not be carried out. In the tenth case, both the Laue symmetry has been increased and a center of symmetry has been added, and the structure further refined.

Introduction

We have come across a number of examples – some recent, some older – of crystal-structure determinations in which the chosen space group was of unnecessarily low symmetry. As has been our custom (Marsh & Herbstein, 1988), we group the corrections to these space groups into two categories: (1) Change in Laue group; in such cases, the original coordinates should conform to the higher symmetry within their e.s.d.'s, and no significant changes in bond lengths or angles should result. (2) Addition of a center of symmetry within the same Laue group; in these cases, much larger coordinate shifts are usually involved, and where possible we have carried out additional refinements in the higher-symmetry centrosymmetric space group. One example belongs to both categories.

In correcting these structures, we find three especially interesting examples. In one case, the original structure

was seriously in error, the NO_3^- counterion having been misplaced due, apparently, to unfortunate misprints in the published coordinates. In a second case, large errors in the measured cell dimensions – several times larger than the indicated precisions – presumably led the authors to assume a triclinic rather than a monoclinic unit cell, whereas the structure itself obeys monoclinic symmetry well within the e.s.d.'s of the coordinates. In a third case the proper rhombohedral unit cell was undetected, perhaps because of its extreme obliquity (the angle α is only 11.24°).

Category 1: change in Laue group

PbAl_2O_4 and PbGa_2O_4

The structures of these two isomorphous compounds (Plötz & Müller-Buschbaum, 1982) were described as triclinic, space group $P1$, $Z = 2$. (PbAl_2O_4 : $a = 5.268$, $b = 8.458$, $c = 5.070$ Å, $\alpha = 90.0$, $\beta = 118.78$, $\gamma = 90.0^\circ$; PbGa_2O_4 : $a = 5.387$, $b = 8.575$, $c = 5.220$ Å, $\alpha = 90.0$, $\beta = 118.99$, $\gamma = 90.0^\circ$; no e.s.d.'s reported.) The authors noted that the cell dimensions for both compounds correspond to centered orthorhombic lattices, but that they were unable to derive a satisfactory structure either in an orthorhombic space group or in the monoclinic space group $P2_1$. In fact, the coordinates for both compounds agree well with space group $Ama2$, No. 40 ($a' = b$, $b' = 2a + c$, $c' = -c$). After suitable transformations ($x' = y$, $y' = \frac{1}{2}x$, $z' = \frac{1}{2}x - z$) and averaging, the coordinates in Table 1 result. The shifts necessary to achieve the symmetry of $Ama2$, included in Table 1, seem satisfactorily small, but no e.s.d.'s are reported so we cannot make a formal comparison. Interatomic distances are, of course, effectively unchanged.

*Contribute No. 8957.